Wind and Structures, Vol. 6, No. 5 (2003) 387-402
DOI: http://dx.doi.org/10.12989/was.2003.6.5.387

Optimal variables of TMDs for multi-mode buffeting control of long-span bridges

S.R. Chen† and C.S. Cai‡

Department of Civil and Environmental Engineering, Louisiana State University, Baton Rouge, LA 70803, USA

M. Gu‡†

Department of Bridge Engineering, Tongji University, Shanghai 200092, China

C.C. Chang‡‡

Department of Civil Engineering, Hong Kong University of Science and Technology, Clear Water Bay, Kowloon, Hong Kong

(Received September 4, 2002, Accepted September 16, 2003)

Abstract. In the past decades, much effort has been made towards the study of single-mode-based vibration controls with dynamic energy absorbers such as single or multiple Tuned Mass Dampers (TMDs). With the increase of bridge span length and the tendency of the bridge cross-section being more slender and streamlined, multi-mode coupled vibrations as well as their controls have become very important for large bridges susceptible to strong winds. As a simple but effective device, the TMD system especially the semi-active one has become a promising option for such coupled vibration controls. However, despite various studies of optimal controls of single-mode-based vibrations with TMDs, research on the corresponding controls of the multi-mode coupled vibrations is very rare so far. For the development of a semi-active control strategy to suppress the multi-mode coupled vibrations, a comprehensive parametric analysis on the optimal variables of this control is substantial. In the present study, a multi-mode control strategy named "three-row" TMD system is discussed and the general numerical equations are developed at first. Then a parametric study on the optimal control variables for the "three-row" TMD system is conducted for a prototype Humen Suspension Bridge, through which some useful information and a better understanding of the optimal control variables to suppress the coupled vibrations are obtained. This information lays a foundation for the design of semi-active control.

Keywords: buffeting; tuned mass damper; mode coupling; long-span bridge; control.

1. Introduction

Under wind excitations, long-span bridges exhibit complex aerodynamic behaviors. Buffeting

† Graduate Research Assistant
‡ Assistant Professor
‡† Professor
‡‡ Associate Professor

random response induced by the turbulence of airflow happens throughout the full range of wind speeds. As the wind speed increases, aerodynamic instability phenomena such as flutter may occur (Simiu and Scanlan 1996). Much research effort has been made towards mitigating excessive vibrations and improving aerodynamic stabilities for bridges during construction (Conti, *et al*. 1996, Takeda, *et al*. 1998) and at service stages (Gu, *et al*. 1994, Wilde, *et al*. 1999). Among all of the control procedures, dynamic energy absorbers such as tuned mass dampers (TMDs) were studied and adopted in suppressing excessive vibrations or maintaining the flutter stability of bridges (Gu, *et al*. 1998).

In recent years, the importance of aeroelastic modal coupling to the bridge aerodynamic behaviors has been recognized (Tanaka, *et al*. 1993, Bucher and Lin 1988, Lin and Yang 1983, Miyata and Yamada 1999, Cai and Albrecht 2000). It has been concluded that the coupling tendency of modes depends on their mode shapes and natural frequencies in still air as well as the flutter derivatives of the bridge section (Jain, *et al.* 1996). The adoption of more slender deck and the increase of bridge span length tend to result in closer modal frequencies. As a result, modal coupling effects through aeroelastic forces in high wind speeds increase (Jain, *et al.* 1998, Namini, *et al.* 1992, Katsuchi, *et al*. 1998, Thorbek and Hansen 1998).

The TMD is known to be effective in suppressing single-mode resonant vibrations when its frequency is tuned to the modal frequency of the structure. When the modal frequencies of the bridge are well separated and modal coupling effects are weak, each TMD is mainly designed to control a single-mode vibration while the effects from other modes on the control are omitted (Igusa and Xu 1991, Kareem and Kline 1995). Abe and Igusa (1995) studied the performances of TMDs on a coupled system with closely-spaced natural frequencies. Through the assumption of very close frequencies, some analytical studies were carried out to the strongly coupled system. Studies on multi-mode wind-induced vibration controls are limited to the cases with very weak coupling effects (Chang, *et al*. 2003) and few works have focused on the vibration controls of bridges with strong aeroelastic modal coupling.

Considering the complexity of bridge conditions under strong winds, an adjustable TMD system is desirable for the control system to be more robust and effective over various circumstances. However, the effects of system properties on the optimal variables of the TMDs have not been sufficiently addressed. Such study is extremely helpful in evaluating the control performance before the real control devices are designed in practice. It also helps in deciding, for the adaptive control system, what parameters of the bridge-flow system are to be monitored in a feed-back control. With such information, the number of variables to be monitored can accordingly be reduced to the least, through which the cost and complexity of the controller can also be minimized.

In this paper, a comprehensive investigation on the optimal variables of the adjustable TMD system is made. First, a general formulation of the multi-mode buffeting response control with multiple TMDs is developed. Second, a control strategy with “three-row” TMDs is discussed especially to study the coupled vibration controls. Finally, the three most important factors of the bridge-flow system are studied numerically with the Humen Suspension Bridge built in China. This parametric study is conducted to investigate the factors of the bridge-flow system that will affect the optimal variables of TMDs as well as the control efficiency. These analytical results will be very useful in carrying out further studies of adaptive control strategy based on the “three-row” TMD model in order to “smartly” suppress the wind-induced vibrations.

2. Multi-mode coupled vibration control with TMDs

Consider a general case shown in Fig. 1 where a bridge has multiple TMDs, displacement $r(x, t)$, and wind forces consisting of buffeting force $f_b(x, t)$ and aeroelastic self-excited force $f_s(x, r, \dot{r})$. Assuming that a total number of n_1 modes are included in the analysis and a total number of n_2 TMDs are attached to the bridge deck at the location of $x_s(s=1$ to $n_2)$, the equation of motion for the bridge-TMD system can be derived as :

$$\boldsymbol{M}\boldsymbol{\eta}'' + \boldsymbol{C}\boldsymbol{\eta}' + \boldsymbol{S}\boldsymbol{\eta} = \boldsymbol{G} \tag{1}$$

where

$$\boldsymbol{\eta} = \{\xi_1, \cdots \xi_{n_1}, \gamma_1, \cdots \gamma_{n_2}\}' \tag{2}$$

$$\boldsymbol{M} = \begin{bmatrix} M^1_{n_1\times n_1} & M^2_{n_1\times n_2} \\ M^3_{n_2\times n_1} & I_{n_2\times n_2} \end{bmatrix} \tag{3}$$

$$\boldsymbol{C} = \begin{bmatrix} C^1_{n_1\times n_1} & 0 \\ 0 & C^2_{n_2\times n_2} \end{bmatrix} \tag{4}$$

$$\boldsymbol{S} = \begin{bmatrix} S^1_{n_1\times n_1} & 0 \\ 0 & S^2_{n_2\times n_2} \end{bmatrix} \tag{5}$$

$$\boldsymbol{G} = \{Q_b, 0\ldots 0\} \tag{6}$$

ξ=generalized coordinate of the bridge; γ=coordinate of TMDs; a superscript prime "′" represents a derivative with respect to dimensionless time $s=Ut/B$; U=mean velocity of the oncoming wind; t=time; B=bridge width; n_1=number of modes; n_2=number of TMDs; I=unit matrix; and Q_b=generalized buffeting force. The components of the matrices are:

$$C^1_{ij}(\omega) = \frac{2\zeta_i\omega_i\delta_{ij} - \rho_a B^4 \omega Z_{ij}}{\left(1 + \sum_{s=1}^{n_2} \mu^i_s\right)} \qquad (i, j=1\ldots n_1) \tag{7}$$

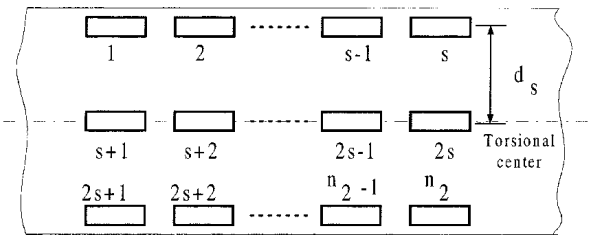

Fig. 1 Overview of the general placement of "three-row" TMDs

$$S_{ij}^{1}(\omega) = \frac{\omega_i^2 \delta_{ij} - \rho_a B^4 \omega^2 T_{ij}}{\left(1 + \sum_{s=1}^{n_2} \mu_s^i\right)} \qquad (i, j=1...n_1) \qquad (8)$$

$$C_{n_2 \times n_2}^{2} = \text{diag}(2\zeta_t^1 \omega_t^1, 2\zeta_t^2 \omega_t^2, \cdots, 2\zeta_t^{n_2} \omega_t^{n_2}) \qquad (9)$$

$$S_{n_2 \times n_2}^{2} = \text{diag}((\omega_t^1)^2, (\omega_t^2)^2, \ldots, (\omega_t^{n_2})^2) \qquad (10)$$

$$M_{ij}^{1} = \frac{I_{ij} + \sum_{s=1}^{n_2} \int_0^l I_t^s r_i(x) r_j(x) dx}{I_{ii}\left(1 + \sum_{s=1}^{n_2} \mu_s^i\right)} \qquad (i, j=1...n_1) \qquad (11)$$

$$M_{ij}^{2} = \frac{\int_0^l I_t^j r_i(x) dx}{I_{ii}\left(1 + \sum_{s=1}^{n_2} \mu_s^i\right)} \qquad (i=1...n_1;\ j=1...n_2) \qquad (12)$$

$$M_{ij}^{3} = r_j(x_i) \qquad (i=1...n_2;\ j=1...n_1) \qquad (13)$$

$$\begin{aligned} Z_{ij} = {} & H_1^* G_{h_i h_j} + H_2^* G_{h_i \alpha_j} + H_5^* G_{h_i p_j} \\ & + P_1^* G_{p_i p_j} + P_2^* G_{p_i \alpha_j} + P_5^* G_{p_i h_j} + A_1^* G_{\alpha_i h_j} + A_2^* G_{\alpha_i \alpha_j} + A_5^* G_{\alpha_i p_j} \end{aligned} \qquad (14)$$

$$\begin{aligned} T_{ij} = {} & H_4^* G_{h_i h_j} + H_3^* G_{h_i \alpha_j} + H_6^* G_{h_i p_j} \\ & + P_4^* G_{p_i p_j} + P_3^* G_{p_i \alpha_j} + P_6^* G_{p_i h_j} + A_3^* G_{\alpha_i h_j} + A_4^* G_{\alpha_i \alpha_j} + A_6^* G_{\alpha_i p_j} \end{aligned} \qquad (15)$$

where δ_{ij}=Kronecker delta function that is equal to 1 if $i=j$ and equal to 0 if $i \neq j$; ω_i and ζ_i=circular natural frequency and mechanical damping ratio of i^{th} mode, respectively; ρ=air density; l=bridge length; H_i^*, P_i^*, A_i^* (i=1−6)=experimentally determined flutter derivatives; ζ_t^s and ω_t^s =damping ratio and circular natural frequency of the s^{th} TMD, respectively; $I_t^s = m_s$ (the mass of the s^{th} TMD) for vertical and lateral bending modes or $I_t^s = m_s \times d_s^2$ (the mass moment of inertia of the s^{th} TMD) for torsion mode; and d_s=horizontal distance between the s^{th} TMD and the torsion

center of the cross-section (see Fig. 1).

The modal integral ($G_{r_i s_j}$) can be expressed as:

$$G_{r_i s_j} = \int_0^l r_i(x) s_j(x) dx \tag{16}$$

and the mass moment of inertia of the bridge section can be expressed as:

$$I_{ij} = \int_0^l m(x) r_i(x) r_j(x) dx \tag{17}$$

where r_i=h_i, p_i or α_i; s_j=h_j, p_j or α_j; $m(x)$=mass per length of the deck for vertical and lateral bending modes; and $m(x)$=mass moment of inertia per length of the deck for torsion mode.

The generalized inertia ratio between the s^{th} TMD and the i^{th} mode, μ_s^i, is defined as:

$$\mu_s^i = \frac{\int_0^l I_t^s r_i^2(x) dx}{I_{ii}} \tag{18}$$

Buffeting force due to the turbulence of wind can be expressed as:

$$L_b = \frac{1}{2}\rho U^2 B\left[C_L\left(2\frac{u}{U}\right) + (C'_L + C_D)\frac{w}{U}\right] \tag{19}$$

$$D_b = \frac{1}{2}\rho U^2 B\left[C_D\left(2\frac{u}{U}\right) + C'_D\frac{w}{U}\right] \tag{20}$$

$$M_b = \frac{1}{2}\rho U^2 B^2\left[C_M\left(2\frac{u}{U}\right) + C'_M\frac{w}{U}\right] \tag{21}$$

where u and w=horizontal and vertical turbulence of wind flow, respectively; and C_L, C_D and C_M= static coefficients of lift, drag and moment of the bridge deck, respectively. A prime over the coefficients represents a derivative with respect to the attack angle.

Eq. (1) can be Fourier transformed into a new format as

$$\boldsymbol{F}\bar{\eta} = \bar{\boldsymbol{G}} \tag{22}$$

where $\bar{\eta}$ and $\bar{G}$=Fourier transformation of η and G, respectively. The impedance matrix $\boldsymbol{F}$ has the general form as $F_{ij} = -\omega^2 M_{ij} + i\cdot\omega C_{ij}(\omega) + S_{ij}(\omega)$, where subscripts i and j=1 to (n_1+n_2) and $i = \sqrt{-1}$.

The mean square of displacements in vertical, lateral and torsion directions can be written as follows:

$$\hat{\sigma}_r^2(x) = \sum_i\sum_j \delta_B^2 r_i(x) r_j(x) \int_0^\infty \tilde{F}_{ij} S_{Q_{b_i}Q_{b_j}} \tilde{F}_{ij}^* dn \tag{23}$$

where; $\tilde{F}_{ij} = [\boldsymbol{F}^{-1}]_{ij}$; $\tilde{F}_{ij} = [\boldsymbol{F}^{-1}]^{*}_{ij}$ and

$$S_{Q_{b_i}Q_{b_j}}(K) = \left(\frac{\rho B^3}{2}\right)^2 \frac{1}{I_{ii}I_{jj}} \int_0^l \int_0^l \{\tilde{q}_i(x_A)\tilde{q}_j(x_B)S_{uu}(x_A, x_B, \omega) + \tilde{r}_i(x_A)\tilde{r}_j(x_B)S_{ww}(x_A, x_B, \omega) + [\tilde{q}_i(x_A)\tilde{r}_j(x_B) + \tilde{r}_i(x_A)\tilde{q}_j(x_B)]C_{uw}(x_A, x_B, \omega) + i \cdot [\tilde{q}_i(x_A)\tilde{r}_j(x_B) - \tilde{r}_i(x_A)\tilde{q}_j(x_B)]Q_{uw}(x_A, x_B, \omega)\} dx_A dx_B \quad (24)$$

$$\tilde{q}_i(x) = 2[C_L h_i(x) + C_D p_i(x) + C_M \alpha_i(x)] \quad (25)$$

$$\tilde{r}_j(x) = (C'_L + C_D)h_j(x) + C'_D p_j(x) + C'_M \alpha_j(x) \quad (26)$$

where S_{uu} and S_{ww}=wind velocity spectrum in the horizontal and vertical direction, respectively; and C_{uw} and Q_{uw}=cross spectrum and quadrature spectrum of u and w (Jain, *et al*. 1996), respectively.

Control efficiency of displacement at the location of x on the bridge span and in the direction of r is defined as

$$R_r(x) = \left(1 - \frac{\hat{\sigma}_r(x)}{\sigma_r(x)}\right) \times 100\% \quad (27)$$

where $\hat{\sigma}_r(x)$ and $\sigma_r(x)$ are the root-mean-square (RMS) of displacement after and before control at the location of x and in the direction of r, respectively; $r=h$, p or α representing vertical, lateral and torsion direction, respectively.

3. "Three-row" TMD model

According to the previous studies on modal coupling, there are only a limited number of modes prone to couple together (Katsuchi, *et al*. 1998). Among all of the coupling cases for streamlined cross sections, the most common modal coupling is between vertical bending mode and torsion mode. Furthermore, in terms of the contribution of individual mode to the total buffeting response as well as the flutter occurrence, the vertical bending and torsion modes usually play the major role. Hence, an appropriate control strategy of TMD system will be developed based on such observed characteristics. It is known that TMDs placed on the center line of the cross section normally have insignificant control effect on the torsion modes. Therefore, we adopt three rows of TMDs: one along the center line of the cross section (named center row hereafter), and other two identical rows along the two sides of the cross section (named side rows hereafter) as shown in Fig. 2. This model is to literally separate the TMD control role into vertical bending and torsion modes since they are the main concern of wind-induced vibrations. In other words, the center row TMD is mainly for vertical mode and the two side rows mainly for torsion mode. Such separation of TMD role is very generic and more valid for the situation when modal coupling effect is weak under low wind speed. As will be found later, side rows of TMD will also contribute to the dynamic suppression of vertical mode in the high wind speed when strong modal coupling exists.

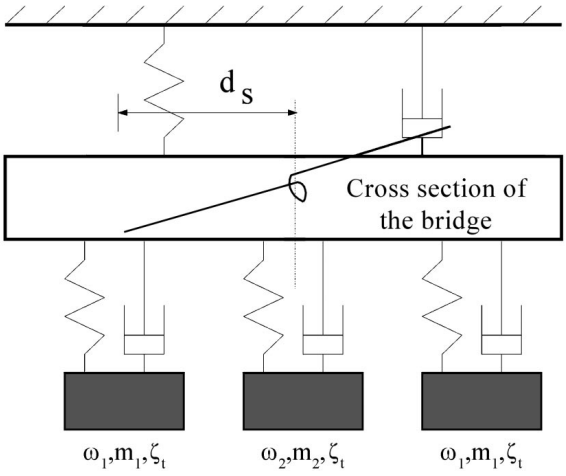

Fig. 2 "Three-row" TMD model

The difference between the multiple-TMD and single-TMD placements is that the multiple placements are more robust in control since they cover a wider range of frequencies (Kareem and Kline 1995, Abe and Fujino 1994). Since the present study is only to disclose the nature of optimal variables for coupled vibration controls, only one TMD in each row is considered to reduce the complexity while without losing the generalities. Also, since the damping ratio of the TMD is not a very sensitive variable for TMD (Gu, *et al*. 1994), damping ratios of all the TMDs are assumed to be the same as ζ_t. The frequency and mass of the two identical TMDs on the side rows are assumed to be ω_1 and m_1, while the frequency and mass of the center TMD are assumed to be ω_2 and m_2 (Figs. 2 and 3), respectively. The total generalized mass of TMDs, greatly related to the efficiency and the cost of the control system, is assumed to be 1% of that of the 1st bending mode of the bridge.

In the present study, two cases are considered in the analysis of the optimal variables of the TMDs. In Case 1, the TMD frequencies ω_1 and ω_2 under a particular wind speed are set to be the optimal values based on single-torsion and single-bending mode vibration controls, respectively. These optimal values were analytically derived by Fujino and Abe (1993). Under the condition of a given total mass of TMDs (1% of the 1st bending mode), the distribution of mass between m_1 and

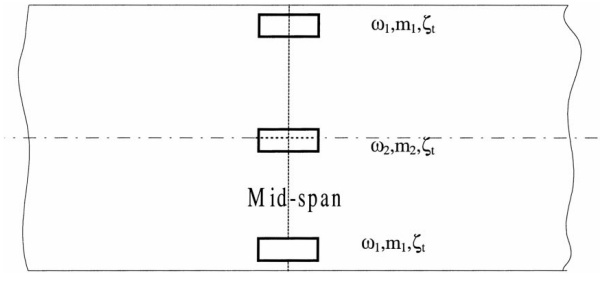

Fig. 3 Overview of the "three-row" TMDs placement for case study of Humen Suspension Bridge

m_2 is varied and studied. This is to simulate the case when the TMD mass can be adjusted while the control objective of each TMD targets a particular mode (e.g., center row for the bending mode and side rows for the torsion mode). In Case 2, the total mass of the two side row TMDs (2 m_1) is set to be equal to the center one (m_2), maintaining the total TMD mass the same as Case 1. Only the variables ω_1, ω_2 and ζ_t can be adjusted. This is to simulate a case that the mass of each TMD is fixed, while the frequency and damping ratio can be adjusted to obtain the optimal control performance.

4. Optimal variables of "three-row" TMDs

Humen Suspension Bridge with a main span of 888 m is chosen as an example here with the basic data shown in Table 1 (Lin and Xiang 1995). A coupled vibration analysis has shown that the 1st symmetric vertical bending mode and the 1st symmetric torsion mode are the two modes most prone to couple together. Therefore, only these two modes, with a modal frequency of 0.17 and 0.36 Hz, respectively, are included in the following analysis. Flutter derivatives H^*_{1-3} and A^*_{1-3} are shown in Fig. 4 (Lin and Xiang 1995). With the increase of wind speed, the modal properties including modal damping and modal frequencies can be obtained using complex eigenvalue approach (Chen and Cai 2003). The results of modal properties are plotted in Fig. 5 and the flutter critical wind speed is identified as 87 m/s for Humen Bridge, which is very close to the result from

Table 1 Main parameters of Humen Bridge

Main span (m)	888	Lift coefficient at 0° attack angle	0.02
Width of the deck (m)	35.6	Drag coefficient at 0° attack angle	0.84
Clearance above water (m)	60	Pitching coefficient at 0° attack angle	0.019
Equivalent mass per length (10^3 *kg/m)	18.34	$(\partial C_L/\partial\alpha)\|_{\alpha=0^o}$	0.51
Equivalent inertial moment of mass per length (10^3 *kg/m)	1743	$(\partial C_M/\partial\alpha)\|_{\alpha=0^o}$	0.62
Structural damping ratio	0.005	d_s (m)	14
Natural frequency of 1st symmetric vertical bending mode (Hz)	0.17	Natural frequency of 1st symmetric torsion mode (Hz)	0.36

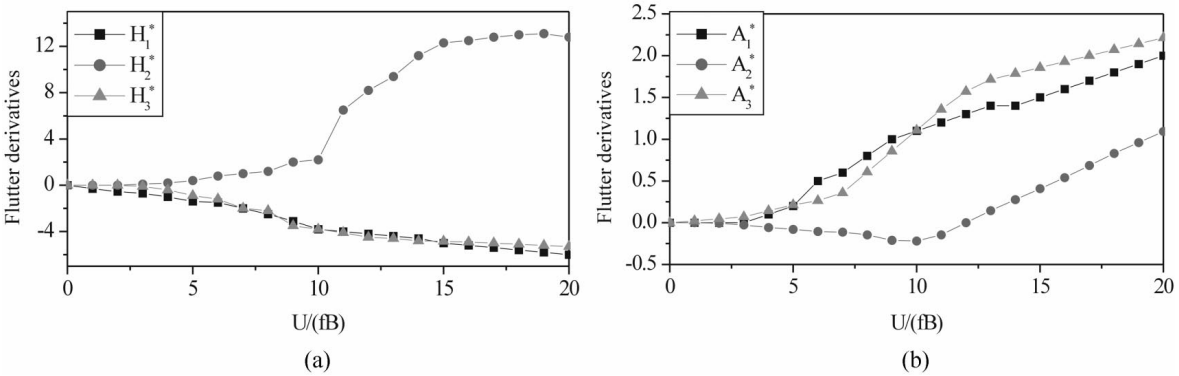

Fig. 4 Flutter derivatives of Humen Suspension Bridge

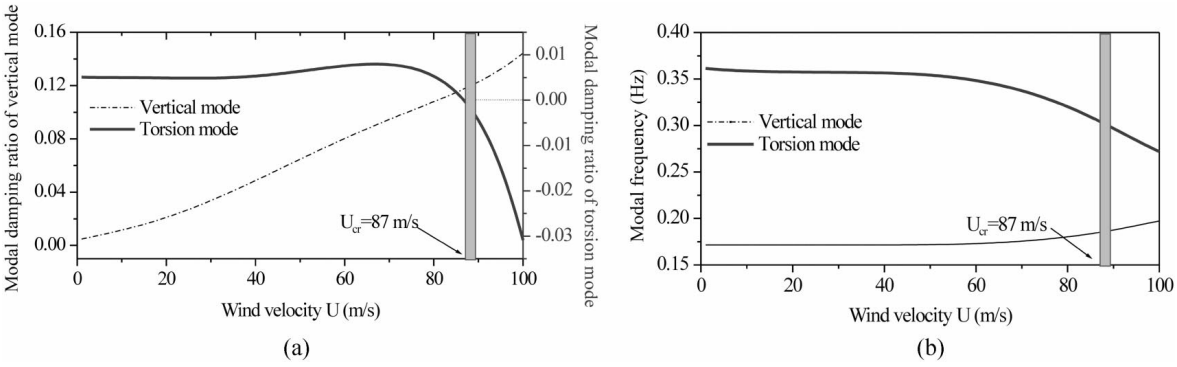

Fig. 5 Variation of modal properties for Humen Suspension Bridge with wind speed

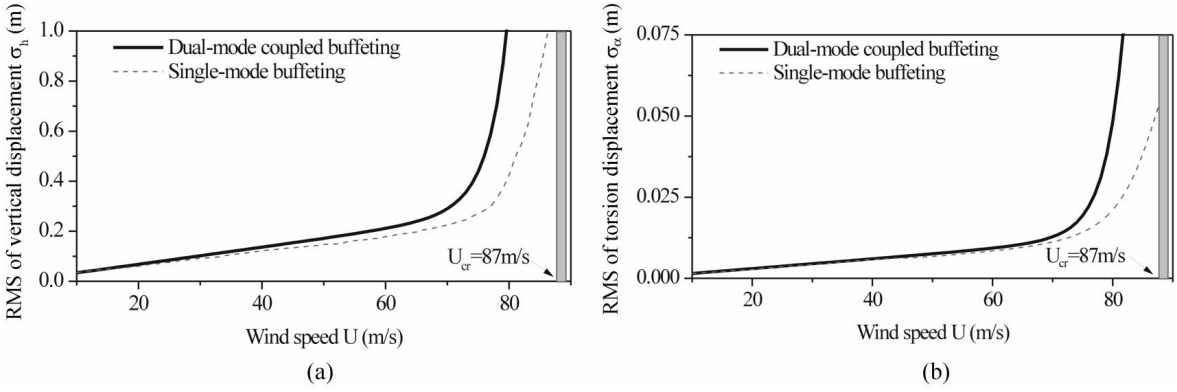

Fig. 6 Buffeting response at the centre of mid-span for Humen Suspension Bridge without control

wind tunnel test (Lin and Xiang 1995). Fig. 6 gives the buffeting response in vertical and torsional directions at the center of the mid-span section without control. Results from coupled analysis based on the two modes (vertical bending and torsion) and from the single- mode analysis are compared. Strong coupling effects in high wind speeds can be observed from that the results of coupling analysis differ obviously from that of single-mode analysis when wind speed is high.

In the following control studies, the chosen location of interests is at the edge of the mid-span section where the largest vertical displacements are expected. The vertical displacement in that location can combine the contributions from the vertical bending mode as well as the torsion mode. The contribution from the torsion mode is calculated with the torsion angle multiplying one-half of bridge width. The TMDs are placed as shown in Fig. 3. The total generalized mass of TMDs, chosen as 1% of that corresponding to the 1st bending mode, is 80,000 kg. For Case 2, the center row and two side rows have the same mass, i.e., $2m_1=m_2=40{,}000$ kg. The horizontal distance from the side row TMD to the center of torsion d_s (Figs. 1 and 2) equals to 14 m for the Humen Bridge.

If only a single-mode-based vibration is considered, the optimal frequency of TMDs at wind velocity 30 m/s can be obtained with formulas by Fujino and Abe (1993) as:

$$\frac{\omega_2}{\omega_h} = 0.99 \tag{28}$$

$$\frac{\omega_1}{\omega_\alpha} = 0.97 \tag{29}$$

where, ω_h and ω_α=natural circular frequencies of vertical and torsion modes, respectively. As discussed earlier, these single-mode-based optimal frequencies are chosen for the TMDs in Case 1.

There exist many factors affecting the coupling effects among modes. From the existing knowledge of the modal coupling, the frequency ratio between the coupling-prone modes and the wind speed are the main possible factors that may affect the optimal variables of TMDs (Katsuchi, *et al*. 1998). The wind speed greatly affects the aeroelastic modal coupling effects and affects the buffeting contribution from coupling-prone modes. These factors are discussed below.

4.1. Effect of wind speed

Aeroelastic coupling is of a great concern in wind-induced vibration of long-span bridges especially when wind speed is quite high. For most streamlined cross sections, the aeroelastic coupling is directly related to the wind speeds. When the total mass of TMDs is fixed as in Case 1, the predicted optimal mass distributions among the TMDs vary significantly for different wind speeds as shown in Fig. 7. At the wind speed of about 60 m/s, the masses of center and side TMDs are about equal ($2m_1/m_{\text{total}} \cong m_2/m_{\text{total}} \cong 0.5$). At lower wind speed (say 40 m/s), much more mass needs to be assigned to m_2 ($m_2/m_{\text{total}} \cong 0.85$) with the bending-single-mode-based optimal frequency. However, at higher wind speed (say 80 m/s), much more mass should be assigned to m_1 ($2m_1/m_{\text{total}} \cong 0.80$) with the torsion-single-mode-based optimal frequency. There are probably two main reasons for such phenomena: one is as the increase of wind speed, the contribution of the torsion mode to the total vertical response at the edge of the mid-span section increases; the other is

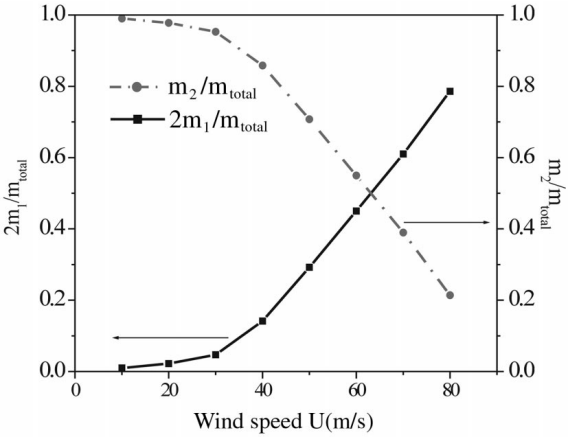

Fig. 7 Optimal mass distribution of TMDs versus wind speed (Case 1)

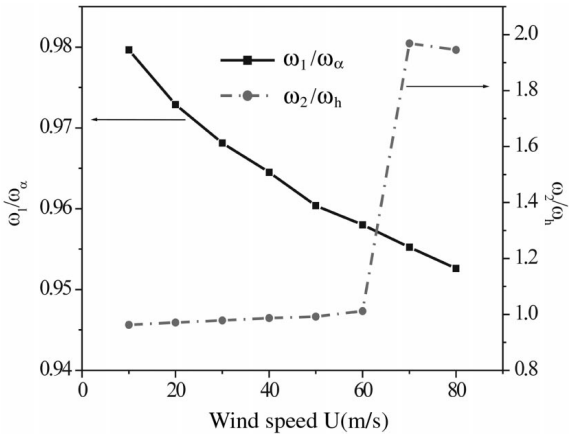

Fig. 8 Optimal frequencies of TMDs versus wind speed (Case 2)

that the resonant part of the bending mode response is difficult to be suppressed due to its large modal damping (Fig. 6). Another part of bending response in high wind speed is due to the modal coupling effects between bending and torsion modes (Chen and Cai 2003), and it can be suppressed with TMD with torsion mode frequency. As stated earlier, the frequencies of TMD are set to be equal to the optimal frequency considering single-mode-based vibrations in Case 1. In terms of vertical response control at the edge of the mid-span section, it is noted that the dominant vibration mode changes from vertical to torsion mode at the wind speed of about 60 m/s.

For Case 2, since the mass of each TMD is fixed, namely $2m_1=m_2$, the optimal frequency changes with the wind speed especially when the wind speed is high as shown in Fig. 8, where ω_h and ω_α are the modal frequencies of bending and torsion modes considered in this study, namely, 0.17 and 0.36 Hz, respectively. Fig. 8 also indicates that with the increase of the wind speed, the optimal frequency of TMD in the center row may change dramatically from around the modal frequency of the bending mode (indicated by $\omega_2/\omega_h=1.0$) to around the torsion mode frequency (indicated by $\omega_2/\omega_h=2.0$ since ω_α is about twice of the bending frequency ω_h). This drastic change occurs at the wind speed of 60 m/s where dominant vibration mode for the vertical response at the edge of the mid-span section changes from bending mode to torsion mode.

Fig. 9 shows the respective optimal damping ratio of TMDs for Case 1 and Case 2. Compared to other variables such as mass distribution and frequency, the damping ratio of the TMDs seems to be less sensitive to the change of wind speed. Therefore, it has relatively the least necessity to be adjusted in an adaptive control.

With the change of wind speed, the optimal control efficiency of the vertical displacement on the edge at the mid-span section. R_h also varies accordingly as shown in Fig. 10. It is observed that the control efficiency decreases with the increase of wind speed until around 60 m/s, where the dominant vibration control mode changes from bending mode to torsion mode. Then, the control efficiency increases with the increase of wind speed. Such phenomenon cannot be observed in a single-mode-based control analysis. Hence, this observation is extremely important for the design of a special controller that, for example, controls bridge vibrations under hurricane-induced strong

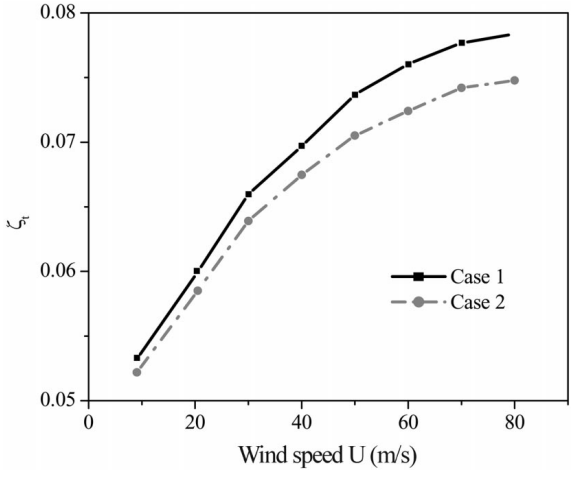

Fig. 9 Optimal damping ratio of TMDs versus wind speed

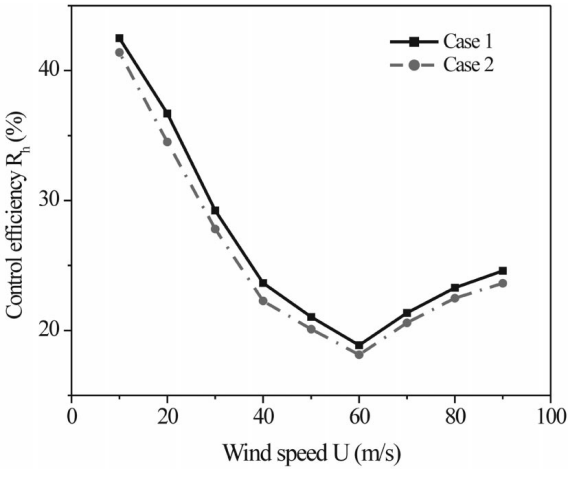

Fig. 10 Optimal control efficiency of "three-row" TMDs versus wind speed

winds. An ideal TMD system in this case should target the bending vibration when wind speed is less than 60 m/s and then is adjusted to target the torsion mode vibration.

4.2. Effect of frequency ratio

With an optimal searching of the TMD mass under the condition of a fixed total mass, the optimal distribution of the total mass among the center and side TMDs has been obtained above. By numerically varying the torsion/bending modal frequencies ratio of the bridge, the effects of the bridge frequency ratio on the TMD optimal variables are studied below considering the wind speed of 30 m/s. It should be noted that for Case 1, the ratios between the TMD and the bridge modal frequencies are fixed as shown in Eqs. (28) and (29), i.e., fixed to the optimal frequency for the single-mode-based vibration control. Therefore, the numerical values of the TMD frequencies ω_1 and ω_2 vary with the change of the natural frequencies ω_h and ω_α accordingly.

Fig. 11 shows that the optimal mass of each TMD depends on the frequency ratio between the torsion and bending modes ω_α/ω_h. When the value of ω_α/ω_h is around 1.15, $2m_1/m_{\text{total}}$ is approximately equal to m_2/m_{total}. When ω_α/ω_h is around 1.76, about 95% of the total mass should be allocated to m_2 (that targets the bending vibration) for the most efficient control.

Fig. 12 shows the optimal frequencies of the TMDs versus the ω_α/ω_h ratio when wind speed is 30 m/s, considering Case 2 where $2m_1=m_2$. It can be found from the figure that the ω_α/ω_h ratio affects the optimal frequency of the TMDs for coupled buffeting control. When the frequencies of bending and torsion modes are well separated (with high ω_α/ω_h values, say 1.6), the optimal frequencies of TMDs shown in Fig. 12 are quite close to those of single-mode-based cases shown in Eqs. (28) and (29). This finding justifies the common assumptions that the control strategy for weakly coupled vibration can be simplified as that of single-mode-based control.

Fig. 13 shows that the optimal damping ratio of the TMD is also affected by the ratio of ω_α/ω_h for both Cases 1 and 2. With the increase of ω_α/ω_h, the damping ratio of the TMDs approaches to that of single-mode-based case (Fujino and Abe 1993). The control efficiency of the vertical buffeting vibration (the total vertical displacement from both the vertical vibration of the bending mode and the rotation

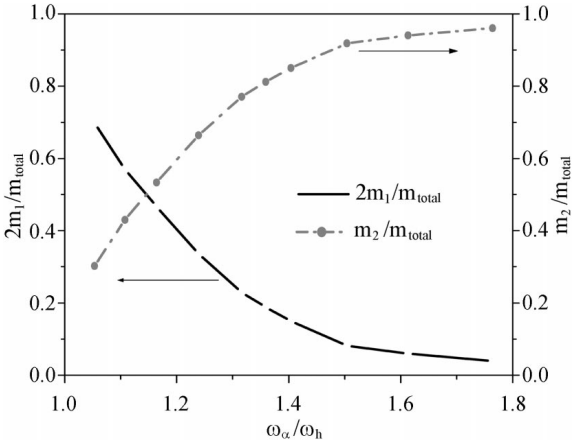

Fig. 11 Optimal mass distribution of TMDs versus frequency ratio of coupled modes (Case 1)

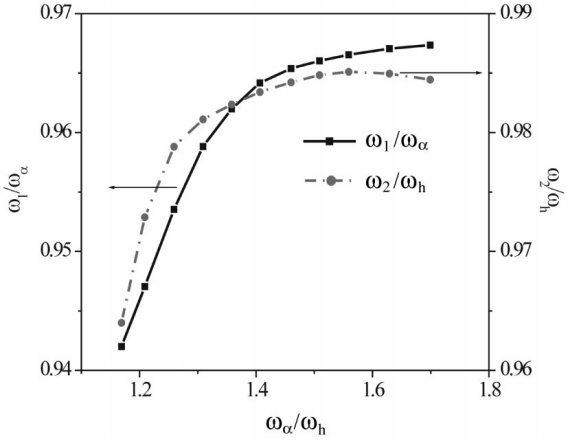

Fig. 12 Optimal frequencies of TMDs versus frequency ratio of coupled modes (Case 2)

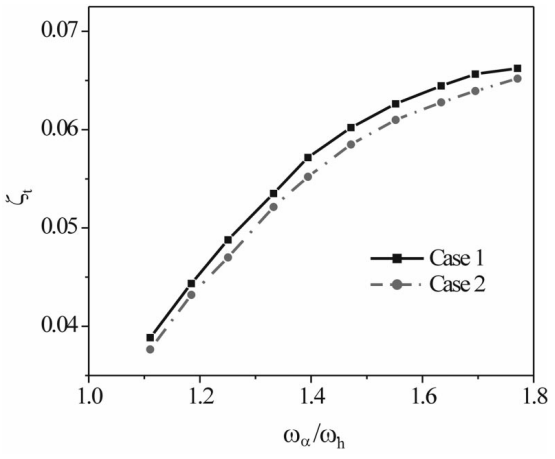

Fig. 13 Optimal damping ratio of "three-row" TMDs versus frequency ratio of coupled modes

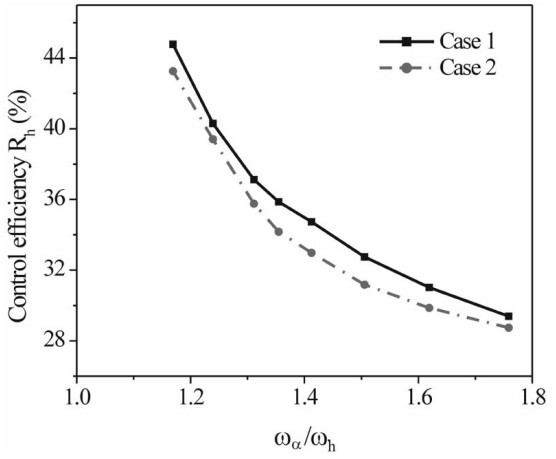

Fig. 14 Optimal control efficiency of "three-row" TMDs versus frequency ratio of coupled modes

of the torsion mode) at the edge of the mid-span section is shown in Fig. 14. With the increase of ω_α/ω_h, the control efficiency decreases and approach to that of a single-mode-based control.

The results discussed above show that the "three-row" TMD control system has the collaborative control effect for the vibration when the frequencies of coupling-prone modes are close, i.e., when the ratio of ω_α/ω_h is low. It has been found that when the ratio of ω_α/ω_h is low, the difference of the optimal variables for the multi-mode-based and those for single-mode-based controls is significant. When the modal frequencies are well separated (with high ω_α/ω_h values), both the optimal variables and control efficiency approach to those of single-mode-based controls. In this case, the TMDs can be designed based on the single-mode control without significantly scarifying the accuracy compared to that of multi-mode based control.

4.3. Effect of modal contributions

Different buffeting response contributions among modes actually indicate the energy distributions of modes and can be varied through changing the static force coefficients in the buffeting force terms, Eqs. (19) to (21). To simulate the relative contributions among modes, the static force coefficient C_m that is related to the contribution of torsion mode is increased numerically with an amplification factor β. Through changing the quantity of buffeting force for torsion mode, the relative contribution to buffeting response among modes can be adjusted. Again, the wind speed is fixed at 30 m/s in the following discussions.

Fig. 15 shows the optimal mass distributions of the TMDs versus the amplification factor β. With the increase of the torsion mode contribution due to the increase of β, the optimal mass m_1 that is mainly responsible for the control of torsion mode response increases. The mass of TMD for torsion mode ($2m_1$) is the same as that for bending mode (m_2) when β is about 7. It can also be found in Fig. 15 that when β approaches 20, essentially all the mass should be assigned to side rows in order to control the vibrations from the torsion mode. When β is less than 3, majority of the mass should be assigned to center row in order to control the vibration from the bending mode at the given wind velocity of 30 m/s.

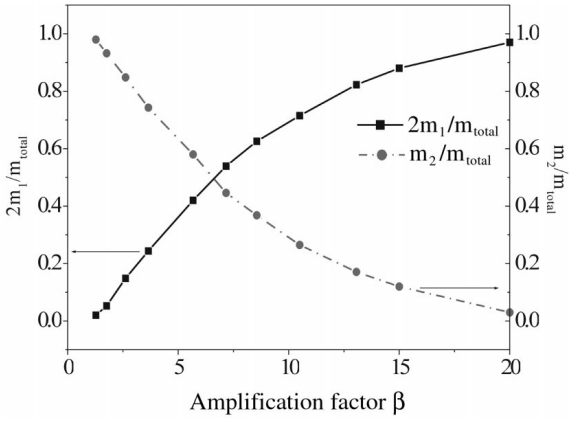

Fig. 15 Optimal mass distribution of TMDs versus amplification factor β (Case 1)

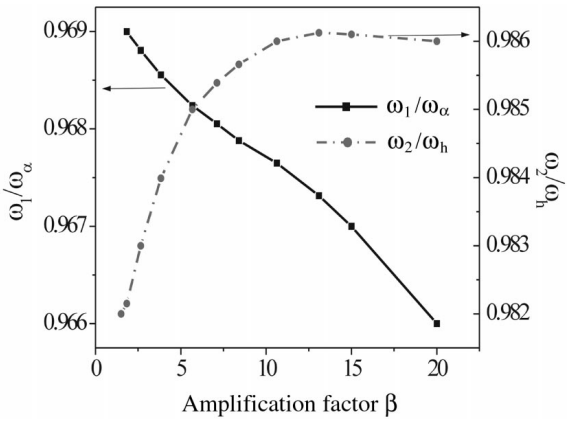

Fig. 16 Optimal frequencies ratio of TMDs versus amplification factor β (Case 2)

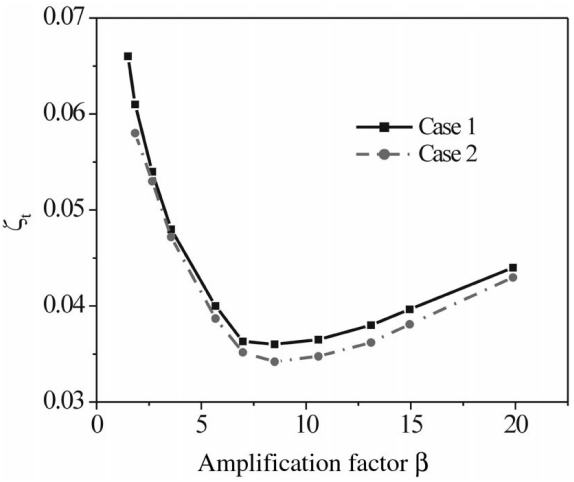

Fig. 17 Optimal damping ratio of "three-row" TMDs versus amplification factor β

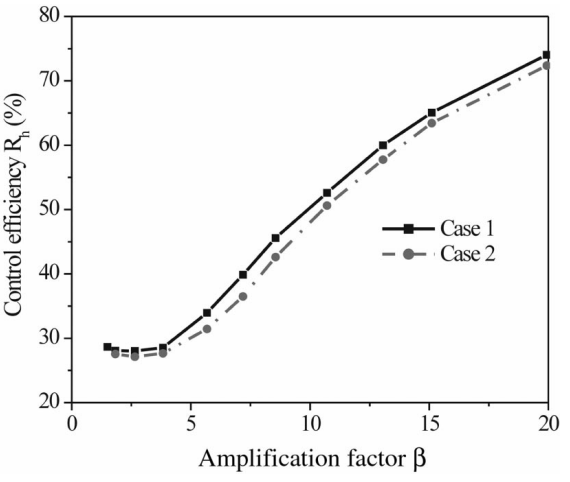

Fig. 18 Optimal control efficiency of "three-row" TMDs versus amplification factor β

Fig. 16 shows the dependency of the optimal frequencies ratio ω_1/ω_α and ω_2/ω_h on the factor β. With the increase of the β, ω_2/ω_h increases from about 0.982 up to about 0.986 and keeps stable, while ω_1/ω_α decreases from about 0.969 to 0.966. These variations are essentially insignificant.

Fig. 17 shows the optimal damping ratio of the TMDs versus β. Since the damping ratio of the TMDs has relatively insignificant effect on the control efficiency of the whole control system, such a variation range of the optimal damping ratio is not that critical. Fig. 18 shows that with the optimal variables of TMDs, the control efficiency increases quickly with the increase of buffeting contribution of the torsion mode, i.e., the increase of β. This implies, for this particular case, that the buffeting response induced by the torsion mode is easier to control compared with that induced by bending mode.

In summary, different modal contributions of the buffeting vibrations has less significant effect on

the optimal frequency and damping ratio if the mass of each TMD is fixed. On the other hand, the optimal mass for each row varies with the change of the contribution factor β, meaning that mass allocation among rows depends on the contribution factor β to some extent. Different bridges have different contributions of buffeting response from each individual mode. Since other variables depend less significantly on the contribution factor β, perhaps only the mass allocation should be made specifically for each bridge. Such feature is helpful to build a general control scheme with robust control performance for different bridges.

5. Conclusions

The mathematical formulation of the bridge-TMD system is developed and a "three-row" TMD strategy is discussed. In this strategy, conceptually, the center TMDs are mainly to control the vibration from bending modes and the side TMDs are for the vibration from torsion modes. However, in high wind speed when strong modal coupling effect exists, the side TMDs will also suppress the coupling part of the bending mode response. The optimal variables of the TMDs are predicted based on multi-mode coupled vibrations, instead of single-mode-based mode-by-mode analysis. The following conclusions can be drawn through the present study:

(1) Wind speed has significant effect on the optimal variables of TMDs, especially when wind speed is high. To efficiently control buffeting vibration over a wide range of wind speeds, an adaptive semi-active TMD control system that can adjust the optimal variables is necessary.

(2) The modal frequency ratio between the torsion and bending modes has large effect on the optimal frequencies of the TMDs as well as the mass distribution when the total mass of the TMDs is fixed. When the frequencies of the coupling-prone modes are close, the optimal variables of the TMDs based on multi-mode coupled vibration control are significantly different from those of single-mode-based control. In these cases, a specific design for coupled vibration control should be considered. When the frequencies of the coupling-prone modes are well separated (weakly coupled vibrations), the optimal variables of the TMDs are close to those of single-mode-based control. In this case, a control strategy based on the single-mode vibration can be used in practice.

(3) The change of buffeting response contribution from the torsion and bending modes has relatively less significant effect on the optimal frequency and damping ratio of the TMDs, while it has significant effect on the mass distribution among the "three-row" TMDs.

(4) The present finding verifies the common assumption that single-mode-based control strategy can be used for bridges with well-separated modal frequencies. However, for coupling-prone bridges with low frequency ratio, the control strategy should be based on the analysis of coupled vibrations. Many modern long-span bridges may fall in this category.

References

Abe, M. and Fujino, Y. (1994), "Dynamic characterization of multiple tuned mass dampers and some design formulas", *Earthquake Eng. Struct. Dynamics*, **23**(8), 813-835.

Abe, M. and Igusa, T. (1995), "Tuned Mass Dampers for structures with closely spaced natural frequencies", *Earthquake Eng. Struct. Dynamics*, **24**(2), 247-266.

Bucher, C.G. and Lin, Y.K. (1988), "Stochastic stability of bridges considering coupled modes", *J. Eng. Mech., ASCE*, **114**(12), 2055-2071.

Cai, C.S. and Albrecht, P. (2000), "Flutter derivatives based random parametric excitation aerodynamic analysis",

Computers & Structures, Elsevier Science, Ltd, UK, **75**(5), 463-477.
Chang, C.C., Gu, M. and Tang, K.H. (2003), "Tuned mass dampers for control of suspension bridges in dual-mode buffeting vibration", *J. Bridge Eng., ASCE*, **8**(4), 237-240.
Chen, S.R. and Cai, C.S. (2003), "Evolution of long-span bridge response to wind-numerical simulation and discussion", *Comput. Struct.*, **81**(21), 2055-2066.
Conti, E., Grillaud, G., Jacob, J. and Cohen, N. (1996). "Wind effects on Normandie cable-stayed bridge: Comparison between full aeroelastic model tests and quasi-steady analytical approach", *J. Wind Eng. Ind. Aerodyn.*, **65**, 189-201.
Fujino, Y. and Abe, M. (1993), "Design formulas for tuned mass dampers based on a perturbation technique", *Earthquake Eng. Struct. Dynamics*, **22**, 833-854.
Gu, M., Chang, C.C., Wu, W. and Xiang, H.F. (1998), "Increase of critical flutter wind speed of long-span bridges using tuned mass dampers", *J. Wind Eng. Ind. Aerodyn.*, **73**(2), 113-123.
Gu, M., Xiang, H.F. and Chen, A.R. (1994), "A practical method of passive TMD for suppressing wind-induced vertical buffeting of long-span cable-stayed bridges and its application", *J. Wind Eng. Ind. Aerodyn.*, **51**, 203-213.
Igusa, T. and Xu, K. (1991), "Vibration reduction characteristics of distributed tuned mass dampers", *Proc. 4th Int. Conf. on Recent Advances in Structural Dynamics*, Southampton, USA, 596-605.
Jain, A., Jones, N.P. and Scanlan, R.H. (1998), "Effect of modal damping on bridge aeroelasticity", *J. Wind Eng. Ind. Aerodyn.*, **77-78**, 421-430.
Jian, A., Jones, N.P. and Scanlan, R.H. (1996), "Coupled flutter and buffeting analysis of long-span bridges", *J. Struct. Eng., ASCE*, **122**(7), 716-725.
Kareem, A. and Kline, S. (1995), "Performance of multiple mass dampers under random loading", *J. Struct. Eng., ASCE*, **121**(SE2), 349-361.
Katsuchi, H., Jones, N.P., Scanlan, R.H. and Akiyama H. (1998), "Multi-mode flutter and buffeting analysis of the Akashi-Kaikyo Bridge", *J. Wind Eng. Ind. Aerodyn.*, **77&78**, 431-441.
Lin, Y.K. and Yang, J.N. (1983), "Multimode bridge response to wind excitation", *J. Eng. Mech., ASCE*, **109**(2), 586-603.
Lin, Z.X. and Xiang, H.F. (1995), "Full scale wind tunnel test of Humen Bridge", Technical report of state key laboratory of wind tunnel in China (in Chinese).
Miyata, T. and Yamada, H. (1999), "New idea on the aero-elastic coupled behavior control of the super long span bridges", *Proc. 2th World Conf. on Structural Control* (Kyoto, Japan 1999), **2**, 843-850.
Namini, A., Albrecht, P. and Bosch, H. (1992), "Finite element-based flutter analysis of cable-suspended bridges", *J. Struct. Eng., ASCE*, **118**(6), 1509-1526.
Simiu, E. and Scanlan, R.H. (1996), *Wind Effects on Structures - Fundamentals and Applications to Design*, John Wiley & Sons Publication.
Takeda, T., Niihara, Y., Ohshio, M., Nakano, R., Kozuma, F. and Ogawa, A. (1998), "Vertical gust response control of long span cable-stayed bridge under cantilever construction by active mass damper", *Proc. of the 2nd World Conference on Structural Control*, 835-842.
Tanaka, H., Yamamura, N. and Dung, N.N. (1993), "Multi-mode flutter analysis and two and three dimensional model test on bridges with non-analogous modal shapes", *J. Struct. Mech. Earthquake Eng.*, Tokyo, Japan, **10**(2), 35-46.
Thorbek, L.T. and Hansen, S.O. (1998), "Coupled buffeting response of suspension bridges", *J. Wind Eng. Ind. Aerodyn.*, **74-76**, 839-847.
Wilde, K., Fujino, Y. and Kawakami, T. (1999), "Analytical and experimental study on passive aerodynamic control of flutter of a bridge deck", *J. Wind Eng. Ind. Aerodyn.*, **80**, 105-119.

AK